Accepted Manuscript

Title: pH Sensitive Dexamethasone Encapsulated Laponite Nanoplatelets: Release Mechanism and Cytotoxicity

Author: <ce:author id="aut0005" author-id="S0378517317300017-adc6e6972b98cef09e8609474f4a6dd9"> M. Roozbahani<ce:author id="aut0010" author-id="S0378517317300017-8de31af3b36d59fa8488ee8f054c7006"> M. Kharaziha<ce:author id="aut0015" author-id="S0378517317300017-9ef485a727f55b25b2c5fbf2ec05aa11"> R. Emadi

PII: S0378-5173(17)30001-7
DOI: http://dx.doi.org/doi:10.1016/j.ijpharm.2017.01.001
Reference: IJP 16333

To appear in: *International Journal of Pharmaceutics*

Received date: 22-11-2016
Revised date: 1-1-2017
Accepted date: 2-1-2017

Please cite this article as: Roozbahani, M., Kharaziha, M., Emadi, R., pH Sensitive Dexamethasone Encapsulated Laponite Nanoplatelets: Release Mechanism and Cytotoxicity.International Journal of Pharmaceutics http://dx.doi.org/10.1016/j.ijpharm.2017.01.001

pH Sensitive Dexamethasone Encapsulated Laponite Nanoplatelets: Release Mechanism and Cytotoxicity

M. Roozbahani[1], M. Kharaziha[1*], R. Emadi[1]

1. Department of Materials Engineering, Isfahan University of Technology, Isfahan 84156-83111, Iran

Corresponding author e-mail: ma.kharaziha@gmail.com

Tel: +98-9133275339

FAX: +98-33912752

Graphical abstract

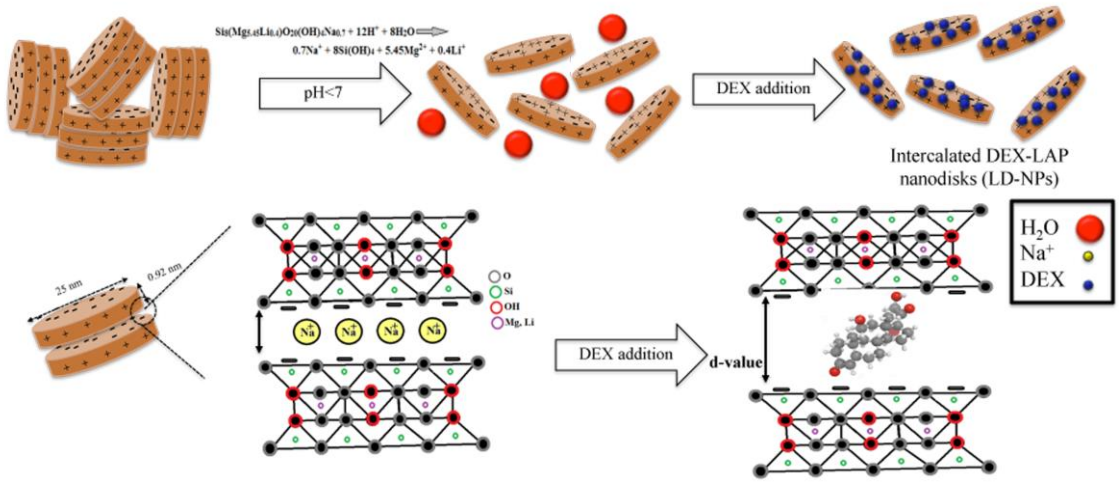

Abstract

The purpose of this study was to develop an efficient strategy to use laponite (LAP) nanoplates as a platform for the efficient release of anionic dexamethasone (DEX). Results revealed that DEX was encapsulated into the interlayer space of LAP nanodisks through an intercalation process with a high loading efficiency of 95.10± 0.80%. XRD patterns as well as FT-IR spectra of the hybrid LAP/DEX nanoplates (LD-NPs) indicated that DEX molecules could successfully adsorb into the LAP nanoplates depending on the pH value. Moreover, in vitro drug release study showed that the release of DEX from LD-NPs was pH-dependent, and DEX released at a faster rate at acidic pH (pH = 5.4) than physiological one. Importantly, MTT (3-(4,5-dimethylthiazol-2-yl)-2,5-diphenyltetrazolium bromide) tetrazolium reduction assay results confirmed that DEX release from LD-NPs not only did not show cytotoxic effect but also improved the viability of MG63 cells compared to LAP-free samples (DEX enriched medium). Our work indicated that LAP nanoplates could be a promising candidate for release of anionic DEX in the controlled manner depending on the pH environment. The merits of LD-NPs such as good cytocompatibility, excellent physiological stability and sustained pH-responsive release properties, make them a promising platform for the delivery of other therapeutic agents beyond DEX.

Keywords: Dexamethasone, Laponite nanoplates, Cytotoxicity, Drug release

1. Introduction:

Dexamethasone (DEX), a synthetic member of the glucocorticoid class of steroid hormones, is an anti-inflammatory and immunosuppressant drug which has been widely applied to treat the inflammatory diseases such as asthma (Wang, Nelin et al. 2008, Sahoo, Panda et al. 2013, Venditti, Fontana et al. 2014), meningitis(Mathur, Garg et al. 2013) and rheumatoid arthritis(Park, Yang et al. 2012). Moreover, DEX molecule plays important roles on the regulation of genes and cellular reactions responsible for the growth and division of cells (Forouzandeh, Hesaraki et al. 2014). It could also promote the differentiation of mesenchymal stem cells (MSCs) toward the osteogenic lineage (Kharaziha, Fathi et al. 2015, Li, Zhou et al. 2015). However, results demonstrated that the direct administration of DEX has been limited mainly due to its toxic and undesirable side effects such as osteoporosis, high sugar concentrations in the blood, hypertension, and stomach and intestinal bleeding due to the ulceration (Jain and Datta 2015, Li, Zhou et al. 2015). The effective dosage range of DEX is approximately 4-20 mg/day and high dosage of DEX is required to reach its therapeutic level in the blood plasma. Therefore, an efficient drug delivery system is desirable to overcome the drawbacks associated with drugs (Jain and Datta 2015). Numerous nanosystems have been considered for administration of DEX consisting of micelles (Hamdi, Lallemand et al. 2015), dendrimers (Choksi, Sarojini et al. 2013), liposomes (Gupta 2011, Maestrelli, Bragagni et al. 2016), inorganic nanoparticles (Hamdi, Lallemand et al. 2015, Soni, Desale et al. 2015), nanogels (Soni, Desale et al. 2015) and nanofibers (Webber, Matson et al. 2012, Kharaziha, Fathi et al. 2015). For instance, Kharaziha *et al.* (Kharaziha, Fathi et al. 2015) encapsulated DEX in poly(ε-caprolactone)(PCL)-forsterite nanofibrous membranes for guided tissue regeneration. Results demonstrated that the proliferation and osteogenic differentiation of stem cells from human exfoliated deciduous teeth (SHED) could be regulated via controlled DEX release process.

In the recent years, nanoclay silicates composed of plate-like polyions are emerging as new vehicles in drug delivery system due to their swelling capability, adsorption, and gel-forming characteristics, as well as their bioactive interface which can accommodate polar molecules and drugs (Viseras, Cerezo et al. 2010). The layered structure of the nanoclay silicates provides enough space to immobilize various kinds of molecules through ion-dipole interaction and physisorption. The accumulated drugs in the interlayer area of the lamellar host could release as a result of diffusion and/or de-intercalation process (Depan, Kumar et al. 2009). Among

these nanoclay silicates, laponite (LAP) nanoplates with disc-shaped morphology (25 nm in diameter and 0.92 nm in thickness) and the empirical chemical formula $Na^{+0.7}[(Mg_{5.5}Li_{0.3})Si_8O_{20}(OH)_4]^{-0.7}$ has emerged as a novel synthetic silicate nanoclay (Ruzicka and Zaccarelli 2011). Results demonstrated LAP nanoplates could encourage the osteogenic differentiation of human MSCs (hMSCs) in the absence of any osteoinductive factor such as bone morphogenetic proteins-2 (BMP-2), making it as an ideal nanomaterial for bone tissue engineering application (Gaharwar, Mihaila et al. 2013). Furthermore, the imperfections of LAP nanoplates induce a negatively charged surface and pH-dependent edge surface charges (positive at pH lower than 9) providing separated layers with large total surface area, which can strongly interact with guest compounds through exchangeable Na^+ in hydrated interlayers or absorbance process (Thompson and Butterworth 1992, Takahashi, Yamada et al. 2005, Li, Maciel et al. 2011). This unique structure stimulates the application of LAP nanoplates as an ideal platform for the encapsulation of cationic drugs, specifically molecules with protonated amino groups, such as tetracyclin(Ghadiri, Hau et al. 2013), doxorubicin (Barraud, Merle et al. 2005) and itraconazole (Jung, Kim et al. 2008) as well as on weak bases (Browne, Feldkamp et al. 1980). For instance, results demonstrated the electrostatic interactions of doxorubicin with LAP nanodisks and formation of nano-complexes with improved bioactivity of the drug (Gonçalves, Figueira et al. 2014). However, minor attention has focused on the immobilization of non-ionic drugs such as DEX on LAP nanoplates.

Herein, we presented a novel hybrid system consisting of LAP nanoplates as a platform to release DEX molecules. We also investigated the effects of pH on the adsorption kinetics of DEX on LAP layers in order to determine the optimal pH for maximized encapsulation of DEX. Furthermore, the effects of pH on the DEX release were investigated. Finally, the effects of DEX release from LAP nanoplates on the cell behavior were evaluated.

2. Material and methods

2.1. Materials

Synthetic silicate nanoplates (Laponite RDS) containing SiO_2 (59.5%), MgO (27.5%), Na_2O (2.8%) and Li_2O (0.8%) with low heavy metals content were purchased from Rockwood Additives Limited, UK. DEX was obtained from Sigma Aldrich (95 % purity). Phosphate buffer saline (PBS) was prepared based on the protocol used in Dulbecco's study (Dulbecco and Vogt 1954).

2.2. Preparation and characterization of LAP/DEX nanoplates (LD-NPs).

In order to optimize LAP concentration for DEX encapsulation, LAP nanoplates were dispersed in deionized (DI) water under sonication (model WUC-D10H, power 770 W) for 15 min with different concentrations (3, 5, and 10 mg/ml). After the addition of DEX (2 mg/ml) to LAP suspensions, they were stirred magnetically for 24 h in order to make LAP swollen and provide LAP/DEX nanoplates (LD-NPs). As prepared LD-NPs were separated by using centrifugation (6000 rpm, 20 min), washed with DI water for 3 times to remove unabsorbed DEX and air dried.

After optimization of LAP concentration, in order to evaluate the effects of pH on the DEX encapsulation, LAP/DEX mixture in PBS was prepared and pH was adjusted at 3, 7 and 13 using 0.1 M HCl and NaOH. As prepared LD-NPs were labeled based on pH value (3, 7, 13) as LD-3, LD-7 and LD-13, respectively. Drug loading efficiency was estimated by measuring the non-immobilized DEX in the supernatant (Ms) and the amount of DEX in washout solutions (Mw) using UV-vis spectrophotometer at the maximum wavelength of DEX absorbance (242 nm) based on the following equations (Eqs. 1-3) (Ghadiri, Hau et al. 2013) :

$$Mt = Mi - (Ms + Mw) \quad (1)$$

$$\text{Encapsulation efficiency} = \frac{M_t}{M_i} \times 100\% \quad (2)$$

$$\text{Loading capacity} = \frac{M_t}{M_n} \times 100\% \quad (3)$$

where M_t is the weight of encapsulated DEX, M_i is the initial weight of DEX added to LAP suspension and Mn is the weight of LD-NPs.

The morphology of the LAP nanoplates and LD-NPs was evaluated using scanning electron microscope (SEM, Philips XL30). Before imaging, LAP nanoplates and LD-NPs were sonicated in ethanol solution to inhibit agglomeration and then gold sputter coated. Moreover, Transmission microscope electron (TEM, Philips EM208S 100 kV, Netherland) was applied to study the morphology and particle size of LAP nanoplates. LAP nanoplates and LD-NPs were analyzed using Fourier transform infrared (FTIR) spectroscopy using Bruker Tensor-27 In the range of 600-4000 cm^{-1}. X-ray diffraction (XRD, X' Pert Pro X-ray diffractometer, Phillips, Netherlands) carried out with CuKa radiation (λ=0.154 nm) at a generator voltage of 40 kV and a current of 40 mA was applied to recognize the chemical composition of LAP and LD-NPs. Furthermore, the distance between the LAP's layers in the LD-NPs was analyzed using XRD patterns using Bragg's equation (Eq. 4):

$$d = \frac{\lambda}{2\text{Sin}\theta} \quad (4)$$

in which λ is the wavelength of the copper anode source (0.154 nm), d stands for the spacing between the scattering laponite's layers, and θ is the diffraction angle.

Zeta potential of the LAP nanoplates and LD-NPs was measured in DI water using a 633 nm laser in a Malvern ZEN3600 (Malvern Instruments, UK). Before experiment, they were dispersed in DI water using 10 min vortexing and ultrasonication (10 min). The refractive index of silicate nanoplatelets was selected as 1.5 (obtained from MSDS of Laponite XLG). Zeta potential measurements were performed with a detection angle of 17 ° and calculated using the Smoluchowsky model for aqueous suspensions.

2.3. In vitro DEX release study

In vitro DEX release from LD-NPs was assessed under different pH conditions (pH= 5.4 and 7.4). Briefly, 6 mg of LD-NPs was dispersed into 2 ml of PBS solution (pH=7.4) and acetic acid buffer solution (pH=5.4). After 10 min vortexing, LD-NPs suspensions were poured in dialysis bags (Sigma Aldrich, molecular weight cutoff= 14,000) and dialyzed in 8 ml PBS solutions in a small container. The samples were kept on the vibratory heater with constant temperature (37 °C). At the pre-determined interval time, 1 ml of PBS from each container was taken out and replaced with fresh PBS solution. Finally, the absorbance of solution was monitored using UV-vis spectrophotometry at 242 nm and the amount of DEX was estimated from the calibration curve of DEX in the same solution.

2.4. Cell Culture

The cytotoxicity of LAP nanoplates and LD-NPs was investigated using MG63 cell line from the National Cell Bank of Iran at the Pasteur Institute. The MG63 cells were cultured in Dulbecco's Modified Eagle Medium (DMEM-low, Bioidea, Iran) containing 10 %(v/v) fetal bovine serum (FBS) (Bioidea, Iran) and 1%(v/v) streptomycin/ penicillin (Bioidea, Iran) at 37 °C in a humidified atmosphere with 5% CO_2. MG63 cells were cultured with a seeding density of 1×10^4 cells per well into a 96-well plate in order to expand the cells until confluence. After a day of culture, free DEX, LAP nanoplate and LD-NPs solutions (with equivalent DEX concentrations) prepared in culture medium, were added to the cells (n=3 per group) and then incubated at 37 ºC. MG63 cell seeded on tissue culture plat without any additive in culture medium was applied as control (TCP). After 24 and 48 h incubation, the cell culture medium was removed, the wells were rinsed with PBS and cell survival rate were evaluated using 3-(4,5-dimethylthiazolyl-2)-2,5-diphenyl tetrazolium bromide (MTT) purchased from Sigma-Aldrich. In this regard, after incubation of the cells with MTT solution (0.5 mg/ml MTT reagent in PBS) for 4 h solution, DMSO was added to dissolve the purple MTT-formazan crystals. Then, the 96-well plates were read at 570 nm by using a Microplate Reader (Bio Rad, Model 680 instruments). Mean and standard deviation of each sample were reported. The relative cell viability was calculated by the following equation (Eq. 5)(Golafshan, Kharaziha et al. 2017):

$$Relative\ cell\ viability\ (\%) = \frac{A_{sample} - A_c}{A_b - A_c} \quad (5)$$

where A_{sample}, A_b and A_c stand for the absorbance of sample, blank (DMSO) and control (TCP), respectively.

2.5. Statistical analysis

Statistical analyses were performed using one-way ANOVA (n≥ 3) and reported as mean ± standard deviation (SD). To determine a statistically significance difference between groups, Tukey's post-hoc test using GraphPad Prism Software (V.6) with a p-value <0.05 was applied to be significant.

3. Results and discussion

3.1. Characterization of LAP/DEX nanoplates (LD-NPs).

LAP nanodisks have been introduced as a promising drug carrier due to its high surface area, well-controlled nanoscale size, and appropriate cellular interaction. Various kinds of drugs and bioactive molecules can be intercalated through cationic exchange in the structure of LAP nanoplates providing hybrid nanomaterials for biomedical applications(Ghadiri, Chrzanowski et al. 2015). On the contrary to other immobilized drugs, DEX is not cationic and, therefore, could not effectively interact with the LAP surface through electrostatic interaction. In this study, the effects of pH on the DEX immobilization on the LAP nanoplates were evaluated.

Before further experiments, LAP concentration in DI water (3, 5 and 10 mg/ml) was optimized at the constant DEX concentration (2 mg/ml) via the encapsulation efficiency and loading capacity evaluation (Eqs. 2 and 3) using UV–vis spectroscopy at 242 nm. The DEX encapsulation efficiency increased from 72.0 ± 8.8% to 76.0 ± 7.2% and 80.0±4.60% when the concentration of LAP nanoplates was 3, 5 and 10 mg/ml, respectively. In other words, loading capacity of DEX enhanced from 12.1 ± 0.01 to 12.7 ± 0.02 and 13.3±0.9% when the concentration of laponite was 3, 5 and 10 mg/ml, respectively. Therefore, given the DEX loading efficiency and loading capacity as well as the aggregation probability of LAP nanodisks in aqueous medium, the concentration of LAP nanoplates was kept constant at 10 mg/ml for further experiments.

Due to the structural properties of LAP nanoplates, pH changes may have critical role on the DEX encapsulation. Fig. 1(A) revealed that increase in pH value of PBS solution from 3 to 13 resulted in changing the milky white color of LAP nanoplate suspensions to brown indicating the strongly sensitivity of DEX to alkaline conditions. The results of UV-vis spectroscopy of pure LAP nanoplates, pure DEX and LD-NPs samples (Fig. 1(B)) clearly confirmed the encapsulation of DEX in LAP nanoplates. Noticeably, all nanohybrids revealed an absorption peak at around 242 nm which was absent in DEX-free LAP nanoplates, confirming the successful loading of DEX in the nanohybrids. However, the intensity of this absorption peaks varied in various

samples depending on pH condition demonstrating various amounts of DEX loading. The effect of pH value (3, 7 and 13) on the encapsulation efficiency and loading capacity of DEX were evaluated. The DEX encapsulation efficiency enhanced with reduction of pH value from 80.0 ± 4.55 % (at LD-7) to 94.0± 0.54 (at LD-13) and 95.10± 0.80% (at LD-3) while loading capacity enhanced from 13.3% (at LD-7) to 15.6± 0.10 (at LD-13) and 16% (at LD-3). Meanwhile, the zeta potential of LAP nanoplates showed a meaningful difference before and after DEX loading depending on pH condition (Fig. 1(C)). While the surface potential of LAP nanoplates and LD-NPs did not significantly change at pH=7, it was reduced to negative values at pH= 3 after DEX loading. According to Fig. 2(A), when suspended in PBS buffer, LAP nanoplates were negatively charged with ζ-potential of −23.1±8.5 mV. While the pH value of solution changed from 7 to 3, the ζ-potential enhanced to positive charge of +36.1± 2.7 mV. However, increase in pH value to 13 did not noticeably change ζ-potential. The positive ζ-potential of LAP nanodisks prepared at pH=3 (LD-3) reduced (7.5 times) by adding anionic DEX molecules to -16.5±8.3 mV which could be due to the electrostatic interaction of DEX molecules with LAP layers. Moreover, the incorporation of DEX into LAP nanoplates at pH=13 resulted in slightly reduced ζ-potential which might be due to hydrogen bonding and physical absorption of DEX into LAP nanoplates.

The encapsulation of DEX within LAP nanoplates in various pH values was determined using FTIR spectroscopy (Fig. 2(B)). FTIR spectrum of pure LAP nanoplates consisted of Si-O stretching vibration and bending vibration located at approximately 1030 and 470 cm^{-1}, respectively (Fatnassi, Solterbeck et al. 2014) . Furthermore, the wide peak appeared at 3440 cm^{-1} and two sharp bands positioned at 2962 and 2886 cm^{-1} could be related to the bending vibration of –OH stretching from free H_2O and CH-stretching vibrations, respectively (Fraile, Garcia-Martin et al. 2016) . The typical band of LAP nanoplates could be detected in the nanohybrids of LD-NPs with the slight shifting to lower wavenumbers. Specifically, -Si-O stretching vibration shifted to 1045 cm^{-1} at LD-3 sample corresponded to the molecular intercalation between LAP and DEX. It is worth noting that, in addition to the characteristic peaks of LAP nanoplates, FTIR spectra of LD-NPs consisted of a few distinctive absorption bands of DEX molecule. Pure DEX spectrum consists of the broad absorption band around 2900–3400 cm^{-1} related to the stretching of aliphatic C-H bonds as well as the absorption band at 1650 cm^{-1} assigned to C=O stretching vibration(Wang, Li et al. 2015) . Compared to pure LAP, LD-3 sample consisted of distinctive band at 1640 cm^{-1} (the peak was indicated in a green box) corresponded to the C=O bond of DEX confirming the efficiently intercalation of DEX within LAP nanoplates.

The intercalation of drug within the LAP nanoplates often leads to the extension of the LAP nanoplates interlayer space (Jung, Kim et al. 2008). In this context, XRD technique may provide useful data which could

disclose the DEX loading mechanism within LAP nanoplates. XRD patterns of DEX molecule, LAP nanoplates as well as LD-NPs are presented in Fig. 2(C). Compared to the XRD pattern of DEX molecules, three main diffraction planes of DEX could be identified in the 2θ range of 15−25° in the XRD patterns of LD-NPs confirming the successful encapsulation of DEX within LAP nanoplates. Moreover, XRD pattern of LAP nanoplates consisted of five well-separated diffraction peaks related to (001), (02,11), (005), (20,13) and (060) diffractions which were similarly reported in previous researches (Jung, Kim et al. 2008, Wang, Zheng et al. 2012) . After DEX encapsulation, the characteristic diffraction peak of LAP nanoplates located at 2θ =6.90° (corresponded to (001) plane) shifted to lower degree, while other peaks did not alter suggesting that LAP could maintain its original crystalline structure after DEX loading (Wang, Wu et al. 2013) . The changes in the position of crystal planes and the distance between the layers of LAP (d-spacing) derived from XRD analysis were calculated from the Bragg' s equation (Eq. 2) and summarized in Table 1. Noticeably, (001) peak significantly shifted (≈16%) to 2θ =6.05° at LD-3, while the distance between the layers of LAP increased (≈15.8%) from 12.81 A° to 14.61 A° demonstrating the DEX loading in LAP nanoplates. Based on previous results, the intercalation of drugs occurred at the reflection peak of (001) plane could be due to the ionic exchange, cation/water-bridging and hydrogen bonding between the two components (Dawson and Oreffo 2013). Moreover, the increase in the d-spacing of LAP nanoplates was the greatest for the LD-3 sample (14.61 °A), revealing that, at this pH, the intercalation of DEX was utmost. Subtracting the thickness of the silicate layer of laponite (9.2 °A) from the d-spacing of samples provided the inter-layer separation distances (Jung, Kim et al. 2008). Results showed that the interlayer distance was about 3.61 °A at pure LAP nanoplates which enhanced to 5.41, 3.63 and 3.69 °A at LD-3, LD-7 and LD-13, respectively. These values were smaller than the longitudinal molecular length of DEX (12.6 °A) suggesting that the absorbed DEX molecules were organized in tilted longitudinal monolayer (Wang, Li et al. 2015). Overall, our XRD results proposed the successful intercalation of DEX within LAP nanoplates via ion exchange at pH=3 condition.

According to the schematic illustrated in Fig. 3, LAP nanoplates consisted of two tetrahedral silica sheets sandwiched one octahedral magnesia sheet. In the middle of octahedral sheets, some of magnesium atoms could be substituted by lithium atoms leading to the deficiency of positive charge within the sheets. The electron rich faces of LAP nanoplates could share the electrons with sodium atoms that reside in the interlayer space in dry condition. During dispersion in the aqueous media, Na^+ ions dissociate leading to the permanent negative charge (non-pH-dependent) to the faces of LAP nanoplates. In other words, the presence of Mg-OH groups from the octahedral magnesia sheets led to formation of pH-dependent edge. According to the pH of medium, either H^+

or OH^- ions could disassociate from the edges rendering the negative or positive charge, respectively. Based on this construct, various types of biomolecules consisting of DEX could interact with inter-particle places, surface position and inter-layer pores of LAP nanoplates based on hydrophobic interactions, hydrogen bonding, cation exchange, proton transfer, cation bridging and anion exchange mechanisms depending on the ambient pH, and the size and electrostatic properties of the interacting molecule (Dawson and Oreffo 2013). In acidic condition (such as pH=3), due to leaching OH^- out and proton transfer, the charge of pH-dependent edge becomes more positive. Therefore, higher encapsulation efficiency of LD-3 might be described by their higher positively charge of edges and less negative surface charge which resulted in the electrostatic interaction between DEX and LAP nanoplates as well as cation-bridging and hydrogen bonding occurred during the dispersion. This behavior was similarly reported for DEX loaded montmorillonite (Forteza, Galan et al. 1989). The authors explained this behavior via the protonated form of the Si-OH groups of the crystal borders, favoring hydrogen bonding between DEX carbonyl groups and the clay surface. Several studies reported that the high surface area of clay nanoparticles could be the main reason to uptake drugs into clay. Drugs could be intercalated (Webber, Matson et al. 2012, Wang, Maciel et al. 2014, Maestrelli, Bragagni et al. 2016) or adsorbed on to the surface of nanoparticles (Porubcan, Born et al. 1979, Forteza, Galan et al. 1989) depending on the surface charge of drug in the environment. According to previous results, due to the negative charge of the face and edge of LAP nanodisks at natural pH, DEX could be physically adsorbed. Based on our results, DEX loading efficiency could be controlled via changing the pH value of the environment during the encapsulation process. At this condition, DEX molecules might be electrostatically interaction with LAP nanodisk instead of physical absorbance.

Various nanoparticles have been applied as carriers in order to control the release of DEX molecules consisting of layered double hydroxides (LDHs) nanoparticles (Wang, Wu et al. 2013) , montmorillonite (Forteza, Galan et al. 1989), montmorillonite and polylactic-co-glycolic acid (PLGA) (Jain and Datta 2015), silica nanoparticles (De Matos, Piedade et al. 2013) and hydrophilic gold nanoparticles (Venditti, Fontana et al. 2014). Wang et al. (Wang, Wu et al. 2013) encapsulated DEX within LDHs nanoparticles via co-precipitation mechanism and demonstrated the successfully encapsulation of DEX into LDHs nanoparticles via strong electrostatic interactions (Wang, Li et al. 2015). In another study, Datta et al.(Jain and Datta 2015) developed a montmorillonite and polylactic-co-glycolic acid (PLGA) nanocomposites as extended release carrier for DEX. They declared that the highest encapsulation efficiency of DEX in this nanocomposite gained 76 % which was significantly less than that in LAP nanoparticles. Moreover, the results showed that the incorporation of montmorillonite in the polymeric drug particles caused the release of drug over a longer period of time (Jain and

Datta 2015).

The SEM images of pure LAP nanoplates and LD-NPs samples (Fig. 4) confirmed the pH depended DEX encapsulation within LAP nanoplates. Pure LAP nanoplates exhibited disk-shaped morphology which strictly aggregated together (Fig. 4(A)). After encapsulation of DEX, all samples revealed less accumulated particles. Specifically, LD-3 sample (Fig. 4(B)) consisted of LAP nanoplates with enhanced distance between layers and DEX molecules spherically deposited on the surfaces and the rims. TEM image of LD-3 shown in Fig. 5(A) also clearly revealed the DEX molecules were uniformly distributed on the LAP nanoplates confirming that all previous results based on the deposition of DEX on the surface of LAP nanoplates. Moreover, according to the particle size distribution histogram (Fig. 5(B)), LD-3 sample consisted of particles with the size of 42.5± 11 nm. Moreover, according to the SEM images of LD-NPs at pH=7 (LD-7, Fig. 4(C)) and pH=13 (LD-13, Fig. 4(D)), lower amount of DEX molecules could be detected on them, which might be due to lower positive charges and repulsive force between LAP nanoplates and DEX molecules, leading to push DEX molecules off.

3.2. DEX release from LAP/DEX nanoplates (LD-NPs)

The main goal of this study was to control DEX release kinetic in various pH conditions from the LAP nanoplates, which might be beneficial for bone regeneration (Porubcan, Born et al. 1979, Yu, Li et al. 2013). The DEX release behavior of nanohybrids was investigated in PBS at pH 7.4 and 5.4 mimicking the conditions presented at normal physiological environment, and the endolysosome internal milieu (pH=5), respectively (Gonçalves, Figueira et al. 2014). Cumulative DEX release profiles (Fig. 6) revealed that DEX released in a two-step manner during 3 days of incubation. The first step was a burst release followed by a gradual and slow release pattern. At the physiological pH condition (pH = 7.4) (Fig. 6(A)), the released DEX from the LD-NPs prepared at pH=3, 7 and 13 at the first step of process, was 43.3± 9.4%, 59.4±1.7% and 35.6±5.2%, respectively. This burst release profile of DEX from LAP nanoplates was consistent with the results of previous studies on smectite clay carriers and could be due to the release of the drug adsorbed onto the edge of clay particles (Dawson and Oreffo 2013, Ghadiri, Chrzanowski et al. 2015). Due to the large size of DEX molecules, the release of entrapped DEX molecules within the interlayer space of LAP nanoplates was hard. Therefore, the burst release could be ascribed due to surface adsorbed DEX molecules instead of entrapped DEX in the LAP nanoplates. Similarly, in another study, tetracycline (TC) molecules intercalated into LAP layers were released a slow manner due to the formation of a complex between LAP structure and TC molecules (Ghadiri, Chrzanowski et al. 2014). Therefore, significantly higher released DEX from LD-7 at this first step might be due to relatively lower positive charge of the LD-7. A lower positive charge of the LAP nanodisks may increase the

repulsive force between the LAP nanodisks and the negatively charged DEX molecules enabling DEX break away from the clay structure more easily. In the second step, the total amount of released DEX prolonged till day 3 reaching a plateau. At this step, the maximum cumulative release of DEX was 56.5 ± 3.2% for LD-7 nanohybrids followed by for LD-3 (46.9 ± 1.9 %) and LD-13 (39.5 ± 6.0 %) samples.

This result was more noticeable in acidic condition (pH=5) and the cumulative drug release profile of nanohybrids revealed strong pH dependent property (Fig. 6(B)). For instance, while only 46.9 ± 1.9 % of DEX released at pH=7.4 from LD-3 sample, after 3 days of soaking, much faster release behavior could be detected for pH=5.4 and the cumulative DEX release reached up to 76.4±7.7 % for LD-3 sample. This pH sensitive release behavior might be due to mechanism of DEX release from the LAP nanodisks and could play an important role in the therapeutic treatments, as the initial fast release could rapidly afford a therapeutic dose, and the following sustained release could preserve the therapeutic dose for a long-time period (Yan, Chen et al. 2013). The release of loaded DEX from LAP nanodisks could be occurred when the DEX molecules which adsorbed on the surface were substituted with Ca^{2+} and K^{+} cations at quasi-physiology medium, and therefore, substitution of H^{+} with these cations (Ca^{2+} and K^{+}) pushed the DEX molecules out from the LAP nanoplates.

3.3. Cytotoxicity evolution of LAP/DEX nanoplates (LD-NPs)

Biocompatibility of LD-NPs was investigated via their cytotoxicity on the MG63 cells via MTT assay during 24 and 48 h periods of culture. According to Fig. 7, compared to DEX treated culture medium, LD-NPs as well as LAP enriched culture medium significantly ($P<0.05$) enhanced the survivability of MG63 cells, after 1 and 2 days of culture. Noticeably, while the relative viability of cells cultured with medium enriched DEX was about 59.5±10%(control), it was enhanced to 105 ±45%(control) in the presence of medium enriched LD-3, confirming the role of LAP nanodisks to control burst release of DEX. Moreover, the viability of cells cultured with LD-7 enriched medium (89.6 ±3 %(control)) was less than LD-3 treated medium which might be due to the burst release of DEX from LD-7 samples as completely discussed in drug delivery section. Finally, Our findings in cell culture test completely met with the results obtained from the drug delivery in previous section.

4. Conclusion

In summary, we presented a facile approach to develop DEX-loaded LAP nanoplates (LD-NPs) with a sustained DEX release profile for bone tissue engineering applications. In this regard, DEX was successfully interlaced within LAP nanoplates depending on the pH value of solution during the DEX encapsulation process. Noticeably, loading efficiency of DEX at pH=3 was 95.10± 0.80% which was significantly higher than those of

at natural and basic conditions. Moreover, DEX release from LAP nanoplates was also revealed pH-sensitive behavior which made it desirable for controlled release of DEX. Furthermore, DEX release from LD-NPs not only did not reveal any cytotoxic effect, but also could increase the viability of MG63 cells compared to LAP-free samples (DEX enriched medium). Overall, the respectable cytocompatibility of the LD-NPs together with sustained DEX release could make them suitable carriers for local delivery of DEX for bone tissue engineering application.

References

Barraud, L., P. Merle, E. Soma, L. Lefrançois, S. Guerret, M. Chevallier, C. Dubernet, P. Couvreur, C. Trépo and L. Vitvitski (2005). "Increase of doxorubicin sensitivity by doxorubicin-loading into nanoparticles for hepatocellular carcinoma cells in vitro and in vivo." Journal of hepatology **42**(5): 736-743.

Browne, J. E., J. R. Feldkamp, J. L. White and S. L. Hem (1980). "Potential of organic cation-saturated montmorillonite as treatment for poisoning by weak bases." Journal of pharmaceutical sciences **69**(12): 1393-1395.

Choksi, A., K. Sarojini, P. Vadnal, C. Dias, P. Suresh and J. Khandare (2013). "Comparative anti-inflammatory activity of poly (amidoamine)(PAMAM) dendrimer–dexamethasone conjugates with dexamethasone-liposomes." International journal of pharmaceutics **449**(1): 28-36.

Dawson, J. I. and R. O. Oreffo (2013). "Clay: new opportunities for tissue regeneration and biomaterial design." Advanced Materials **25**(30): 4069-4086.

De Matos, M., A. Piedade, C. Alvarez-Lorenzo, A. Concheiro, M. Braga and H. De Sousa (2013). "Dexamethasone-loaded poly (ε-caprolactone)/silica nanoparticles composites prepared by supercritical CO 2 foaming/mixing and deposition." International journal of pharmaceutics **456**(2): 269-281.

Depan, D., A. P. Kumar and R. P. Singh (2009). "Cell proliferation and controlled drug release studies of nanohybrids based on chitosan-g-lactic acid and montmorillonite." Acta Biomaterialia **5**(1): 93-100.

Dulbecco, R. and M. Vogt (1954). "Plaque formation and isolation of pure lines with poliomyelitis viruses." The Journal of experimental medicine **99**(2): 167-182.

Fatnassi, M., C.-H. Solterbeck and M. Es-Souni (2014). "Clay nanomaterial thin film electrodes for electrochemical energy storage applications." RSC Advances **4**(87): 46976-46979.

Forouzandeh, A., S. Hesaraki and A. Zamanian (2014). "The releasing behavior and in vitro osteoinductive evaluations of dexamethasone-loaded porous calcium phosphate cements." Ceramics International **40**(1, Part A): 1081-1091.
Forteza, M., E. Galan and J. Cornejo (1989). "Interaction of dexamethasone and montmorillonite—adsorption-degradation process." Applied Clay Science **4**(5): 437-448.
Fraile, J. M., E. Garcia-Martin, C. Gil, J. A. Mayoral, L. E. Pablo, V. Polo, E. Prieto and E. Vispe (2016). "Laponite as carrier for controlled in vitro delivery of dexamethasone in vitreous humor models." European Journal of Pharmaceutics and Biopharmaceutics **108**: 83-90.
Gaharwar, A. K., S. M. Mihaila, A. Swami, A. Patel, S. Sant, R. L. Reis, A. P. Marques, M. E. Gomes and A. Khademhosseini (2013). "Bioactive silicate nanoplatelets for osteogenic differentiation of human mesenchymal stem cells." Advanced materials **25**(24): 3329-3336.
Ghadiri, M., W. Chrzanowski and R. Rohanizadeh (2014). "Antibiotic eluting clay mineral (Laponite®) for wound healing application: An in vitro study." Journal of Materials Science: Materials in Medicine **25**(11): 2513-2526.
Ghadiri, M., W. Chrzanowski and R. Rohanizadeh (2015). "Biomedical applications of cationic clay minerals." RSC Advances **5**(37): 29467-29481.
Ghadiri, M., H. Hau, W. Chrzanowski, H. Agus and R. Rohanizadeh (2013). "Laponite clay as a carrier for in situ delivery of tetracycline." RSC Advances **3**(43): 20193-20201.
Golafshan, N., M. Kharaziha and M. Fathi (2017). "Tough and conductive hybrid graphene-PVA: Alginate fibrous scaffolds for engineering neural construct." Carbon **111**: 752-763.
Gonçalves, M., P. Figueira, D. Maciel, J. Rodrigues, X. Qu, C. Liu, H. Tomás and Y. Li (2014). "pH-sensitive Laponite®/doxorubicin/alginate nanohybrids with improved anticancer efficacy." Acta biomaterialia **10**(1): 300-307.
Gupta, A. S. (2011). "Nanomedicine approaches in vascular disease: a review." Nanomedicine: Nanotechnology, Biology and Medicine **7**(6): 763-779.
Hamdi, Y., F. Lallemand and S. Benita (2015). "Drug-loaded nanocarriers for back-of-the-eye diseases-formulation limitations." Journal of Drug Delivery Science and Technology **30**: 331-341.
Jain, S. and M. Datta (2015). "Oral extended release of dexamethasone: Montmorillonite–PLGA nanocomposites as a delivery vehicle." Applied Clay Science **104**: 182-188.
Jung, H., H.-M. Kim, Y. B. Choy, S.-J. Hwang and J.-H. Choy (2008). "Itraconazole–Laponite: kinetics and mechanism of drug release." Applied Clay Science **40**(1): 99-107.
Jung, H., H.-M. Kim, Y. B. Choy, S.-J. Hwang and J.-H. Choy (2008). "Laponite-based nanohybrid for enhanced solubility and controlled release of itraconazole." International journal of pharmaceutics **349**(1): 283-290.
Kharaziha, M., M. H. Fathi, H. Edris, N. Nourbakhsh, A. Talebi and S. Salmanizadeh (2015). "PCL-forsterite nanocomposite fibrous membranes for controlled release of dexamethasone." Journal of Materials Science: Materials in Medicine **26**(1): 1-11.
Li, L., G. Zhou, Y. Wang, G. Yang, S. Ding and S. Zhou (2015). "Controlled dual delivery of BMP-2 and dexamethasone by nanoparticle-embedded electrospun nanofibers for the efficient repair of critical-sized rat calvarial defect." Biomaterials **37**: 218-229.
Li, Y., D. Maciel, H. Tomás, J. Rodrigues, H. Ma and X. Shi (2011). "pH sensitive Laponite/alginate hybrid hydrogels: swelling behaviour and release mechanism." Soft Matter **7**(13): 6231-6238.
Maestrelli, F., M. Bragagni and P. Mura (2016). "Advanced formulations for improving therapies with anti-inflammatory or anaesthetic drugs: A review." Journal of Drug Delivery Science and Technology **32**: 192-205.
Mathur, N., A. Garg and T. Mishra (2013). "Role of dexamethasone in neonatal meningitis: a randomized controlled trial." The Indian Journal of Pediatrics **80**(2): 102-107.
Park, J. S., H. N. Yang, S. Y. Jeon, D. G. Woo, M. S. Kim and K.-H. Park (2012). "The use of anti-COX2 siRNA coated onto PLGA nanoparticles loading dexamethasone in the treatment of rheumatoid arthritis." Biomaterials **33**(33): 8600-8612.
Porubcan, L. S., G. S. Born, J. L. White and S. L. Hem (1979). "Interaction of digoxin and montmorillonite: mechanism of adsorption and degradation." Journal of pharmaceutical sciences **68**(3): 358-361.
Ruzicka, B. and E. Zaccarelli (2011). "A fresh look at the Laponite phase diagram." Soft Matter **7**(4): 1268-1286.

Sahoo, P., H. Panda and D. Bahadur (2013). "Studies on the stability and kinetics of drug release of dexamethasone phosphate intercalated layered double hydroxides nanohybrids." Materials Chemistry and Physics **142**(1): 106-112.
Soni, K. S., S. S. Desale and T. K. Bronich (2015). "Nanogels: An overview of properties, biomedical applications and obstacles to clinical translation." Journal of Controlled Release.
Takahashi, T., Y. Yamada, K. Kataoka and Y. Nagasaki (2005). "Preparation of a novel PEG–clay hybrid as a DDS material: dispersion stability and sustained release profiles." Journal of controlled Release **107**(3): 408-416.
Thompson, D. W. and J. T. Butterworth (1992). "The nature of laponite and its aqueous dispersions." Journal of Colloid and Interface Science **151**(1): 236-243.
Venditti, I., L. Fontana, I. Fratoddi, C. Battocchio, C. Cametti, S. Sennato, F. Mura, F. Sciubba, M. Delfini and M. V. Russo (2014). "Direct interaction of hydrophilic gold nanoparticles with dexamethasone drug: loading and release study." Journal of colloid and interface science **418**: 52-60.
Viseras, C., P. Cerezo, R. Sanchez, I. Salcedo and C. Aguzzi (2010). "Current challenges in clay minerals for drug delivery." Applied Clay Science **48**(3): 291-295.
Wang, G., D. Maciel, Y. Wu, J. o. Rodrigues, X. Shi, Y. Yuan, C. Liu, H. Tomás and Y. Li (2014). "Amphiphilic polymer-mediated formation of laponite-based nanohybrids with robust stability and pH sensitivity for anticancer drug delivery." ACS applied materials & interfaces **6**(19): 16687-16695.
Wang, S., Y. Wu, R. Guo, Y. Huang, S. Wen, M. Shen, J. Wang and X. Shi (2013). "Laponite nanodisks as an efficient platform for doxorubicin delivery to cancer cells." Langmuir **29**(16): 5030-5036.
Wang, S., F. Zheng, Y. Huang, Y. Fang, M. Shen, M. Zhu and X. Shi (2012). "Encapsulation of amoxicillin within laponite-doped poly (lactic-co-glycolic acid) nanofibers: preparation, characterization, and antibacterial activity." ACS applied materials & interfaces **4**(11): 6393-6401.
Wang, W.-R., A. Li, W. Mei, R.-R. Zhu, K. Li, X.-Y. Sun, Y.-C. Qian and S.-L. Wang (2015). "Dexamethasone sodium phosphate intercalated layered double hydroxides and their therapeutic efficacy in a murine asthma model." RSC Advances **5**(30): 23826-23834.
Wang, X., L. D. Nelin, J. R. Kuhlman, X. Meng, S. E. Welty and Y. Liu (2008). "The role of MAP kinase phosphatase-1 in the protective mechanism of dexamethasone against endotoxemia." Life sciences **83**(19): 671-680.
Webber, M. J., J. B. Matson, V. K. Tamboli and S. I. Stupp (2012). "Controlled release of dexamethasone from peptide nanofiber gels to modulate inflammatory response." Biomaterials **33**(28): 6823-6832.
Yan, L., W. Chen, X. Zhu, L. Huang, Z. Wang, G. Zhu, V. Roy, K. Yu and X. Chen (2013). "Folic acid conjugated self-assembled layered double hydroxide nanoparticles for high-efficacy-targeted drug delivery." Chemical Communications **49**(93): 10938-10940.
Yu, W. H., N. Li, D. S. Tong, C. H. Zhou, C. X. C. Lin and C. Y. Xu (2013). "Adsorption of proteins and nucleic acids on clay minerals and their interactions: A review." Applied Clay Science **80**: 443-452.

Figure caption:

Fig. 1. A) Photographs of LAP suspensions in DI water at various pH values of environment. The color of suspension changed from milky at pH=3 to brown color at pH=13. B) UV-vis spectra of pure LAP nanoplates and DEX as well as LD-NPs hybrids, and C) Changes of zeta potential of DL-NPs, before and after loading DEX.

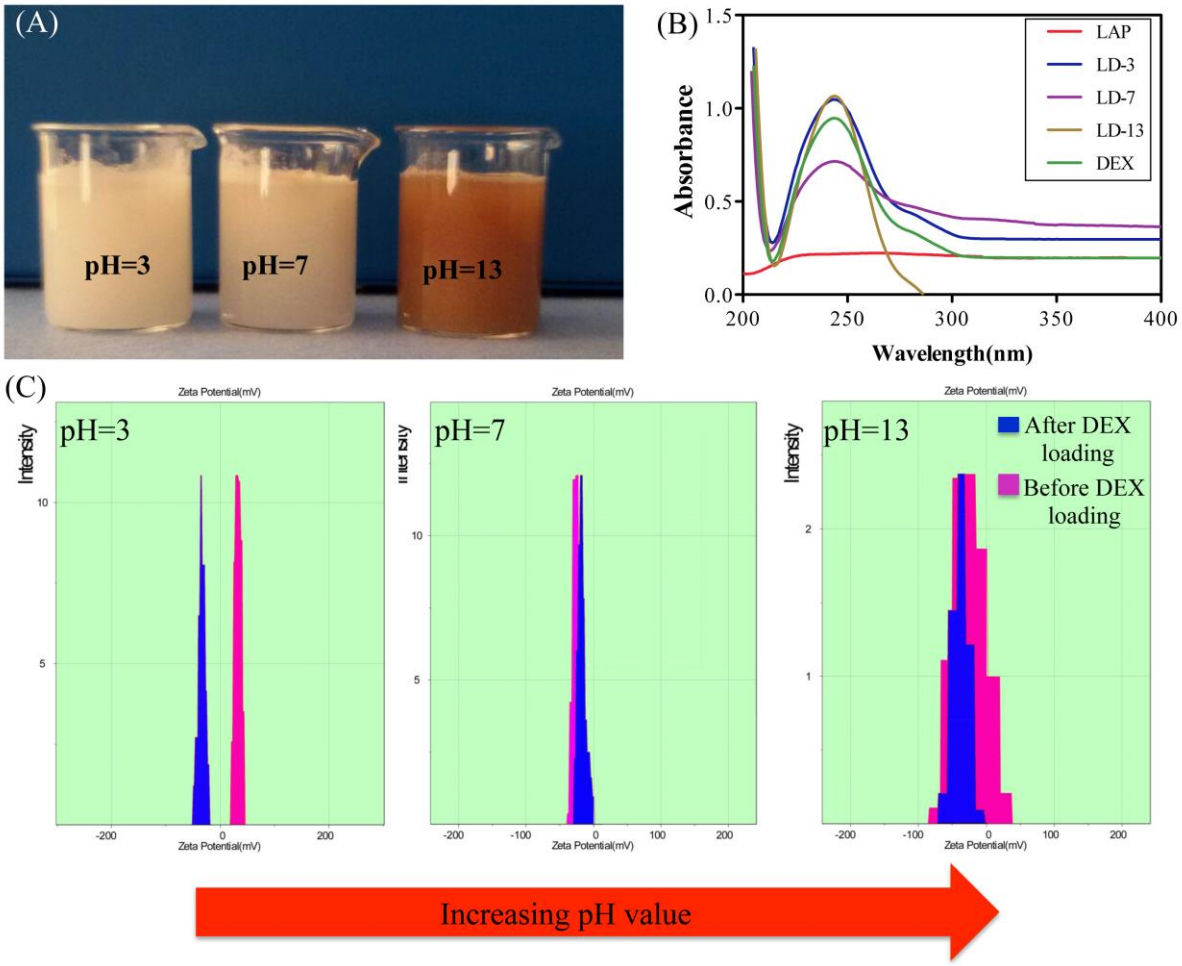

Fig. 2. A) Zeta potential values of LAP nanoplates and LD-NPs at various pH conditions, B) FTIR spectra, and, and C) XRD patterns of pure LAP, DEX, LD-NPs.

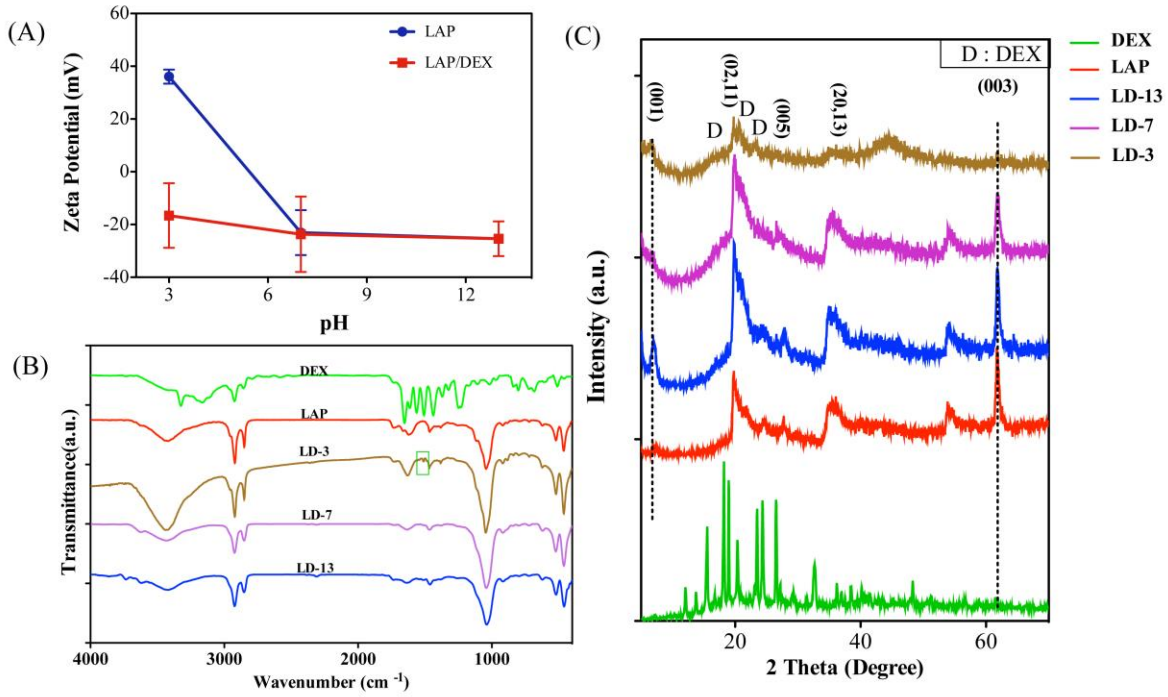

Fig. 3. The schematic illustrating the intercalation of DEX into LAP nanoplates at pH=3

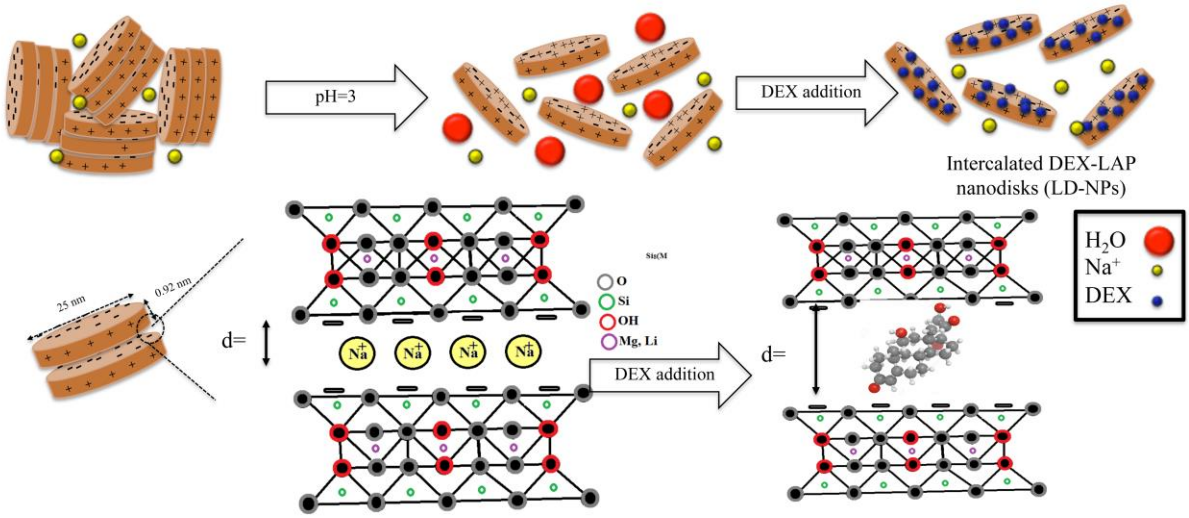

Fig. 4. SEM images of A) pure LAP, B) LD-3, C) LD-7, and D) LD-13 at two different magnifications.

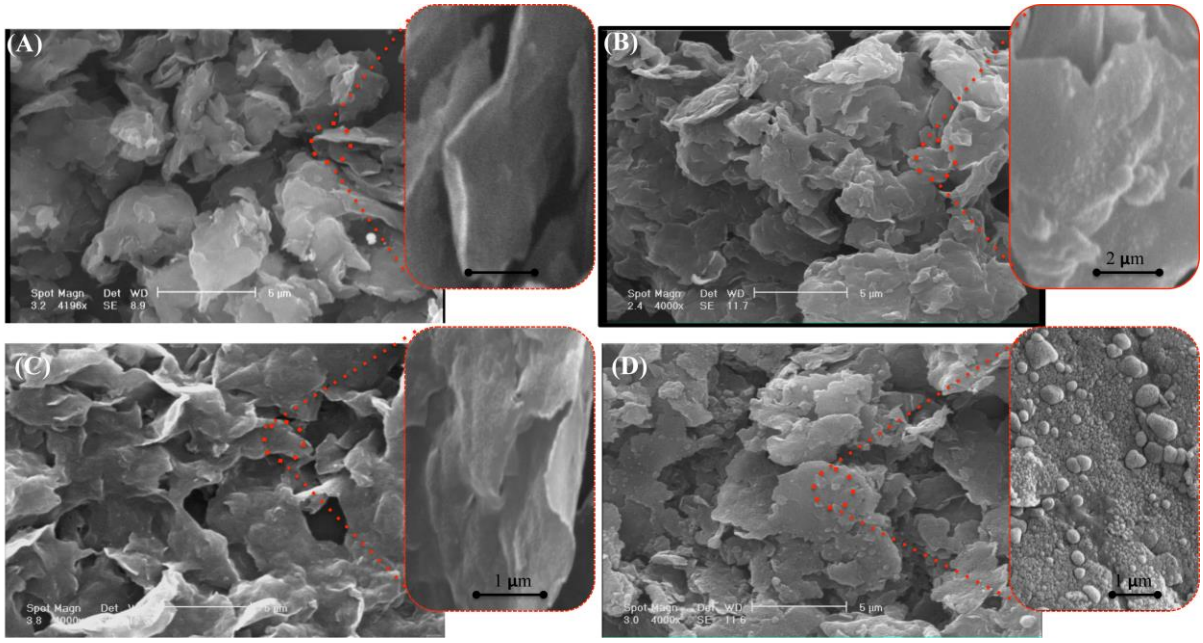

Fig. 5. A) TEM micrograph of LD-3 nanohybrid as well as, B) its average particle size of LD-3.The red arrows indicates the DEX particles uniformly distributed on the surface of nanodisks.

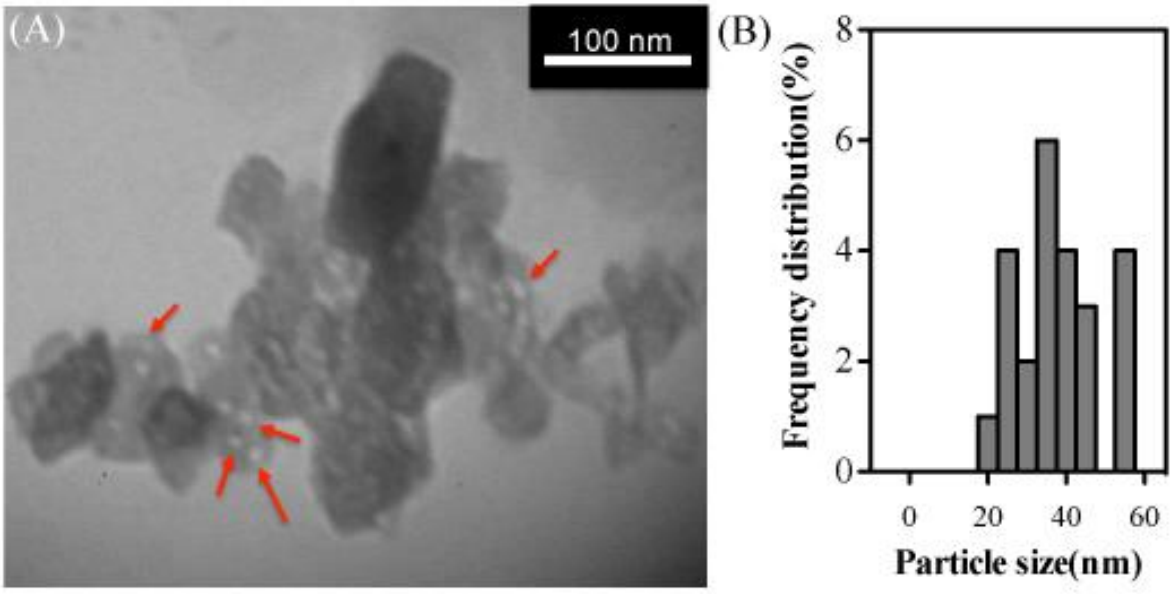

Fig. 6. In vitro cumulative release of DEX from LD-NPs at 37 °C under different pH conditions: A) pH=7.4 and B) pH=5.4

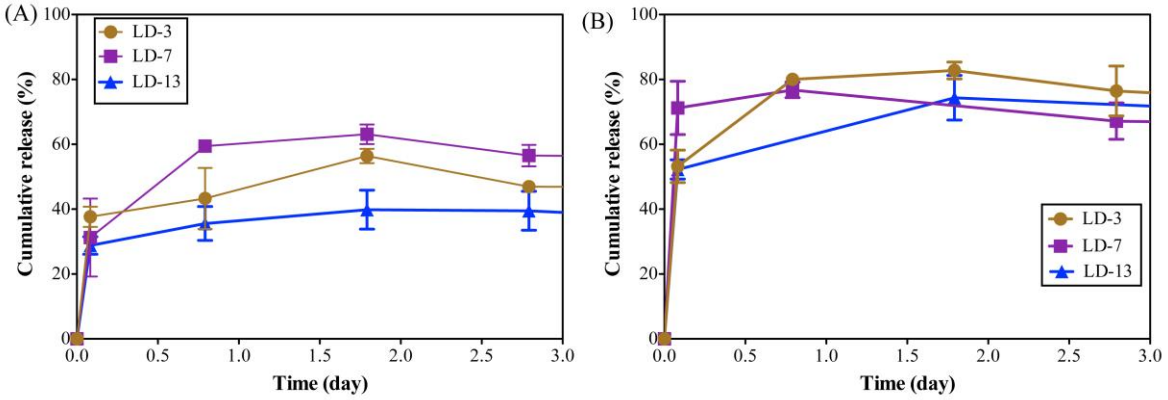

Fig. 7. In vitro MTT viability assay of MG63 cells treated with DEX, LAP nanodisks and LD-NPs for (a) 24 h and (b) 48 h. (* and **: significant difference compared to DEX and LD-13 treated samples, respectively)($P<0.05$).

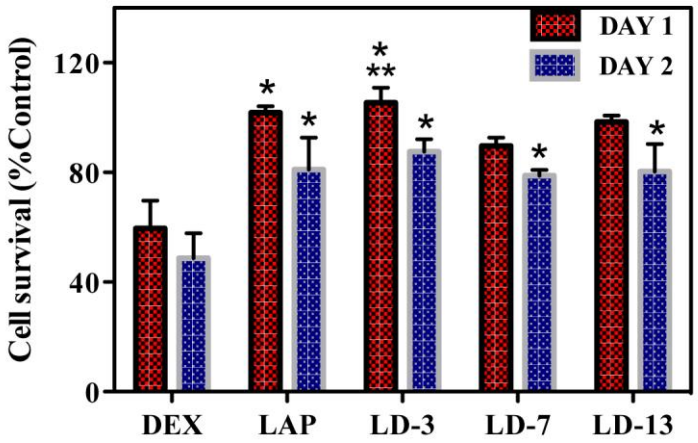

Table 1. 2θ of reflection plans and d-spacing related to pure LAP nanoplates and LAP/DEX extracted from XRD analysis prepared at different pHs.

Reflection plans (hkl)	2θ of reflection plan (degree)				d-spacing (A°)			
	LAP	LD-NPs			LAP	LD-NPs		
		LD-3	LD-7	LD-13		LD-3	LD-7	LD-13
(001)	6.90	6.05	6.89	6.86	12.81	14.61	12.83	12.89
(02,11)	19.84	19.77	19.87	19.87	4.47	4.49	4.47	4.47
(005)	35.10	35.17	35.20	35.11	2.56	2.55	2.54	2.55
(20,13)	554.10	-	54.15	54.16	1.69	-	1.69	1.69
(060)	61.82	61.78	61.90	61.82	1.50	1.50	1.50	1.50